

Novel Glass-Forming Organic Materials. 1. Adamantane with Pendant Cholesteryl, Disperse Red 1, and Nematogenic Groups

Shaw H. Chen,* John C. Mastrangelo, and Hongqin Shi

Department of Chemical Engineering, Gavett Hall University of Rochester, Rochester, New York 14627-0166, and Laboratory for Laser Energetics, 250 East River Road, University of Rochester, Rochester, New York 14623-1299

A. Bashir-Hashemi and Jianchang Li

Geo-Centers, Inc. at ARDEC, 762 Route 15 South, Lake Hopatcong, New Jersey 07849

Nathan Gelber

Armaments Research, Development & Engineering Center, Picatinny Arsenal, New Jersey 07860-5000

Received May 2, 1995; Revised Manuscript Received July 29, 1995*

ABSTRACT: Adamantane was employed as an excluded-volume core for the synthesis of two- and four-arm liquid crystalline, as well as amorphous, molecular systems capable of vitrification upon thermal quenching. It was found that (-)-cholesterol as the side arm exhibited a smectic A and a cholesteric mesophase, whereas 1-phenyl-2-(6-cyanonaphth-2-yl)ethyne and cyanotolan showed a nematic mesophase in both two- and four-arm systems. Furthermore, disperse red 1 resulted in amorphous, nonmesogenic materials. In general, the four-arm systems tend to elevate T_g and T_c and to depress recrystallization of the quenched glass upon heating in comparison to the two-arm systems. It was also found that with 1-phenyl-2-(6-cyanonaphth-2-yl)ethyne, the four-arm adamantane showed an elevated T_g but a somewhat depressed T_c relative to the three-arm cyclohexane counterpart.

I. Introduction

In recent years, one has witnessed intensive research activities targeting amorphous as well as liquid crystalline organic materials for a wide variety of advanced optical applications based on active and passive device concepts. Generically, molecular structures which incorporate functional moieties and which possess desired morphologies are designed largely on an empirical basis for intended applications. Because of their inherent ability to vitrify, polymers containing functional moieties as part of the backbone structure or as a pendant group have been intensively investigated. Although various techniques for processing functional polymers have been established (*e.g.*, spin coating, solvent casting, etc.), low molar mass systems have emerged as a viable alternative in view of their low viscosity, which facilitates solution or melt processing. Moreover, low molar mass systems are amenable to specialized techniques for thin film (*i.e.* ≤ 100 nm) preparation, such as physical vapor deposition,¹ molecular beam epitaxy,² and the Langmuir-Blodgett method.³

From a fundamental perspective, the understanding of vitrification by low molar mass organic compounds has not advanced to a level adequate for offering as a molecular design tool. Because of the potential these materials hold for practical applications, numerous low molar mass materials have been synthesized and demonstrated to vitrify upon quenching but with a varying tendency to recrystallize upon heating across the glass transition temperature,⁴⁻¹⁰ T_g . However, there appears to be a lack of common theme underlying the reported empirical molecular design approaches. In an attempt to furnish a unifying concept, it was proposed that functional moieties be chemically bonded to proper

excluded-volume cores, resulting in essentially hybrid systems comprising structurally disparate constituents. As a consequence, a series of glass-forming, low molar mass materials with superior morphological stability have been successfully synthesized using cyclohexane as a central core.¹¹⁻¹⁴ Being a more rigid and bulkier tricyclic core than cyclohexane, adamantane offers an opportunity to further investigate the effect of central core on vitrification by the resulting hybrid molecular system. The present work was further motivated by a series of recent observations that the adamantane core is capable of elevating T_g in polymeric and low molar mass systems owing to its unique geometric characteristics.¹⁵⁻¹⁷ Specifically, functional moieties such as (-)-cholesterol, disperse red 1 (DR1), and nematogens were attached to 1,3-adamantanedicarboxylic and 1,3,5,7-adamantanetetracarboxylic cores with an objective of evaluating glass-forming abilities of the resultant amorphous and mesogenic molecular systems.

II. Experimental Section

Reagents and Chemicals. All reagents and solvents were received from Aldrich Chemical Company. Most of them were used without further purification: (-)-cholesterol (99%+), 1,3-adamantanedicarboxylic acid (98%), triphenylphosphine (99%), diethyl azodicarboxylate (97%), disperse red 1 (*i.e.*, 2-[N-ethyl-N-(4-[(4-nitrophenyl)azo]phenyl)amino]ethanol, 30 wt % in a binder), anhydrous pyridine (99.8%), methylene chloride (>99.5%), acetone (99.7%). Triethylamine (99%) was dried over 4 Å molecular sieve, and tetrahydrofuran was dried by refluxing over sodium spheres in the presence of benzophenone.

Purification of Disperse Red 1. Disperse red 1 as a precursor to **II** and **VI** was isolated from a commercially available mixture by first adding methylene chloride (75 mL) to disperse red 1 (30% in a binder, 3 g total). The insoluble binder was then removed by filtration, and the crude DR1 was obtained upon evaporating off the solvent *in vacuo*. Further purification was accomplished by recrystallization from ethanol to give dark red crystals (0.8 g). An HPLC analysis showed

* Author to whom correspondence should be addressed.

† Abstract published in *Advance ACS Abstracts*, October 1, 1995.

Table 1. Elemental Analysis of I–VII

compound	I			II			III			IV			V			VI			VII		
	%C	%H	%N	%C	%H	%N	%C	%H	%N	%C	%H	%N	%C	%H	%N	%C	%H	%N	%C	%H	%N
calculated	78.22	9.38	0.00	64.69	5.92	13.72	79.59	5.19	3.44	77.90	6.01	3.63	77.66	9.24	0.00	62.56	5.38	14.96	78.81	4.59	3.75
observed	77.98	9.38	0.00	64.54	6.03	13.57	79.30	5.09	3.49	77.31	6.05	3.68	77.36	9.28	0.00	62.27	5.42	14.74	78.68	4.75	3.72

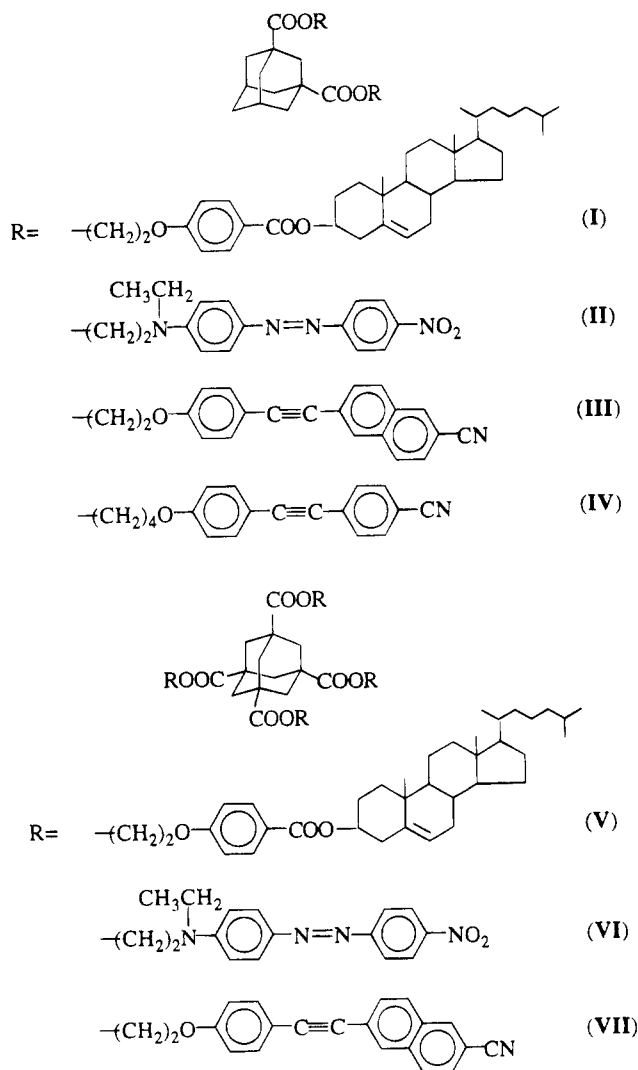


Figure 1. Chemical structures of model compounds I–VII synthesized for the present study.

a purity of better than 99%, and the chemical structure was found to be consistent with the proton NMR spectral data: δ 1.30 (t, 3H, NCH_2CH_3), δ 1.70–2.00 (br, 1H, HOCH_2CH_2), δ 3.55–3.70 (m, 4H, $\text{N}(\text{CH}_2\text{CH}_2\text{CH}_2)$), δ 3.95 (t, 2H, HOCH_2CH_2), δ 6.85 (d, 2H, aromatic *H* ortho to amine), δ 7.95 (m, 4H, aromatic *H* ortho to $\text{N}=\text{N}$), and δ 8.35 (d, 2H, aromatic *H* ortho to NO_2). The DSC thermogram revealed a crystalline melting point at 165 °C with an enthalpy of melting of 88 J/g.

Material Synthesis. The model ester compounds identified in Figure 1 for this study were synthesized by reacting precursor alcohols with 1,3-adamantanedicarboxylic acid to yield I–IV and with 1,3,5,7-adamantanetetracarboxylic acid chloride to yield V–VII, as accomplished previously.^{11,12,14} These model compounds are named as follows: 1,3-adamantanedicarboxylic acid, bis[2-4-[(3 β -5-cholestenyloxy)carbonyl]phenoxy]ethyl ester (I); 1,3-adamantanedicarboxylic acid, bis[2-[N-ethyl-4-[(4-nitrophenyl)azo]phenyl]amino]ethyl ester (II); 1,3-adamantanedicarboxylic acid, bis[2-4-[(6-cyanonaphth-2-yl)ethynyl]phenoxy]ethyl ester (III); 1,3-adamantanedicarboxylic acid, bis[4-4-[(4'-cyanophenyl)ethynyl]phenoxy]butyl ester (IV); 1,3,5,7-adamantanetetracarboxylic acid, tetrakis[2-4-[(3 β -5-cholestenyloxy)carbonyl]phenoxy]ethyl ester (V); 1,3,5,7-adamantanetetracarboxylic acid, tetrakis[2-[N-ethyl-

N-4-[(4-nitrophenyl)azo]phenyl]amino]ethyl ester (VI); 1,3,5,7-adamantanetetracarboxylic acid, tetrakis[2-4-[(6-cyanonaphth-2-yl)ethynyl]phenoxy]ethyl ester (VII).

The precursor alcohol to I and V, *i.e.* 2-4-[(3 β -5-cholestenyloxy)carbonyl]phenoxy]ethanol, was prepared following part of Scheme 2 with attendant procedures as presented in ref 12. Previously reported^{11,12} procedures were followed for the synthesis of 4-4-[(4-cyanophenyl)ethynyl]phenoxy]butanol and 2-4-[(6-cyanonaphth-2-yl)ethynyl]phenoxy]ethanol, *i.e.*, precursor alcohols to III, IV, and VII. The synthesis of 1,3,5,7-tetracarboxymethoxyadamantane was accomplished by photochemical chlorocarbonylation of 1,3-adamantanedicarboxylic acid in an excess of oxalyl chloride as reported elsewhere.¹⁸ A part of the procedures was modified for the preparation of 1,3,5,7-adamantanetetracarboxylic acid chloride by triturating the reaction mixture with cold ether followed by similar work-up procedures to obtain the desired solid product in 40% yield. The proton NMR spectrum (in CDCl_3) showed a singlet at δ 2.25 (s, $\text{C}-\text{CH}_2-\text{C}$).

Characterization Techniques. A Hitachi high-performance liquid chromatography, HPLC, system comprising an L-2000 metering pump and an L-4200 UV–vis absorbance detector equipped with an LiChrosorb column (RP-18, 10 μm) was employed to determine the number of components and purity of the intermediates and products. The purity levels of all final products were found to be better than 99% on the basis of HPLC analysis. Chemical structures were elucidated with elemental analysis (performed by Oneida Research Services, Inc. in Whitesboro, NY), the FTIR (Nicolet 20 SXC), and proton NMR (QE-300, GE) spectroscopic techniques. Stability against thermal decomposition and phase-transition temperatures were determined by thermogravimetric analyzer, TGA, and differential scanning calorimeter, DSC, respectively (DuPont 951 and 910 interfaced with Thermal Analyst 2100 System and DSC-7, Perkin-Elmer) with a continuous nitrogen purge at 50 mL/min. A heating rate of 10 °C/min was consistently employed in TGA experiments, while 5 and 20 °C/min were used in DSC experiments. Morphology and liquid crystallinity were identified with a polarized optical microscope (Leitz Orthoplan-Pol), POM, equipped with a hot stage (FP82, Mettler) plus a central processor (FP80, Mettler).

III. Results and Discussion

The model molecular systems synthesized for the present study are as depicted in Figure 1 with their structures validated by elemental analysis and proton-NMR spectral data compiled in Tables 1 and 2, respectively. From TGA experiments, it was found that no samples showed any weight loss up to 270 °C, which defines the maximum temperature to which samples can be heated without concern for thermal decomposition in the DSC and POM experiments. A standard heating rate of 20 °C/min was adopted for the DSC experiments to reveal any evidence of recrystallization in the organic glasses prepared *in situ* by heating the samples up to 250 °C followed by quenching to –30 °C. To serve as a more stringent test of morphological stability of the quenched glasses, a heating rate of 5 °C/min was attempted in cases where no recrystallization or crystalline melting was observed in the DSC thermograms obtained at 20 °C/min. Although glass transition was readily identified by a step change in the DSC thermogram, the nature of phase and mesophase (*i.e.* first order) transitions was determined by a combination of the texture observed under POM and the enthalpy of transition obtained from DSC experiment.

Table 2. Proton NMR Spectral Data for I–VII: 300 MHz, CDCl₃, δ

I, per repeat unit	II, per repeat unit	III, per repeat unit	IV, per repeat unit	V, per repeat unit	VI, per repeat unit	VII, per repeat unit
0.73–2.47 [m, 50H, $-CH-$, $-CH_2-$ on adamantane ring, and $-CH-$, $-CH_2-$, $-CH_3$ on cholesterol ring]	1.31–2.18 [m, 10H, $-CH-$, $-CH_2-$ on adamantane ring, and $-CH_3$]	1.81–2.22 [m, 7H, $-CH-$, $-CH_2-$ on adamantane ring]	1.75–2.19 [m, 11H, $-CH-$, $-CH_2-$ on adamantane ring, and $-CH_2-$ on cholesterol ring]	0.75–2.48 [m, 46H, $-CH_2-$ on adamantane ring, and $-CH-$, $-CH_2-$, $-CH_3$ on cholesterol ring]	1.24 [s, 3H, $-CH_3$]	2.08 [s, 3H, $-CH_2-$ on adamantane ring]
4.25 [t, 2H, $-CH_2O-$]	3.55 [m, 2H, $-NCH_2-$]	4.25 [t, 2H, $-CH_2O-$]	4.06 [t, 2H, $-CH_2O-$]	4.24 [t, 2H, $-CH_2O-$]	1.88 [s, 3H, $-CH_2-$ on adamantane ring]	4.25 [t, 2H, $-CH_2O-$]
4.46 [t, 2H, $-COOCH_2-$]	3.70 [t, 2H, $-CH_2N-$]	4.50 [t, 2H, $-COOCH_2-$]	4.22 [t, 2H, $-COOCH_2-$]	4.46 [t, 2H, $-COOCH_2-$]	3.46 [m, 2H, $-NCH_2-$]	4.50 [t, 2H, $-COOCH_2-$]
4.85 [m, 1H, $-COOCH-$]	4.33 [t, 2H, $-COOCH_2-$]	6.95–8.23 [m, 10H, arom. H]	6.94–7.67 [m, 8H, arom. H]	4.84 [m, 1H, $-COOCH-$]	3.62 [t, 2H, $-CH_2N-$]	6.94–8.22 [m, 10H, arom. H]
5.44 [m, 1H, $=CH-$]	6.83 [d, 2H, arom. H]			5.43 [m, 1H, $=CH-$]	4.28 [t, 2H, $-COOCH_2-$]	
6.94 [d, 2H, arom. H]	7.94 [m, 4H, arom. H]			6.91 [d, 2H, arom. H]	6.77 [d, 2H, arom. H]	
8.03 [d, 2H, arom. H]	8.34 [d, 2H, arom. H]			8.00 [d, 2H, arom. H]	7.88 [m, 4H, arom. H]	
					8.31 [d, 2H, arom. H]	

Table 3. Phase Transition Temperatures from DSC Second Heating Scans of Quenched Glasses

sample	phase transition temperatures, °C ^{a,b}
I	g 58 S _A 167 Ch 200 I; 156 crystalline 181 melting ^c
II	g 56; 148 crystalline 181 melting ^c
III	g 47 N 89 I ^d
IV	g 17 N 47 I ^d
V	g 86 S _A 236 Ch ^d
VI	g 90 I ^d
VII	g 77 N 190 I ^d

^a TGA thermogram at 10 °C/min showed no weight loss at a minimum temperature of 270 °C for all samples. ^b g: glass transition. N: nematic. S_A: smectic A. Ch: cholesteric. I: isotropic. ^c Both crystallization and crystalline melting peaks were present on second heating scans at 20 °C/min from which glass and mesophase transition temperatures were also determined. ^d No crystallization or crystalline melting observed at heating rates of 5 and 20 °C/min.

From the data summarized in Table 3, the following observations can be made. In general, (–)-cholesterol is expected to induce the formation of the smectic and/or the cholesteric mesophase. In disubstituted adamantane, I, the DSC second heating scan revealed a semicrystalline morphology. Specifically, a glass transition at 58 °C was present followed by a smectic A (focal-conic) to cholesteric (Grandjean steps) transition at 167 °C, as identified under POM, and a clearing point at 200 °C with an enthalpy change of 0.6 J/g. Overlapping with these two mesophase transitions is a recrystallization peak appearing at 156 °C followed by a crystalline melting peak at 181 °C with an enthalpy change of 21.8 J/g. As an approximation, the temperature at the center of the recrystallization peak observed in the DSC thermogram is identified as that giving rise to the maximum crystallization velocity as referred to in previous studies of morphological stability of organic materials.^{4,13} Thus, the ratio of the recrystallization to crystalline melting temperatures (in kelvin), 0.94, falls in the range reported for glass-forming liquid crystals,¹³ 0.93 ± 0.01 . In contrast, in the tetrasubstituted case, V, a higher T_g with a better morphological stability was accomplished in that the semicrystalline character observed in I disappeared. Furthermore, V showed a smectic A (focal-conic) to cholesteric (oil streaks) transition at 236 °C, as identified under POM, with an enthalpy change of 0.3 J/g, but clearing did not occur under POM when heated into the temperature range of thermal decomposition, *i.e.* ≥ 270 °C. Prior to the discussion of systems containing DR1, it should be noted that the *trans*-isomer (at $-N=N-$) has been shown to predominate over the *cis*-isomer.¹⁹ Thus, the *trans* to *cis* geometric isomerism is of no concern regarding its potential effects on morphology as being presently investigated. With DR1 as the pendant group, disubstituted adamantane, II, also yielded a relatively unstable glass with a T_g at 56 °C followed by a recrystallization peak at 148 °C and a crystalline melting peak at 181 °C, again giving a ratio of the recrystallization to crystalline melting temperatures at 0.93 right in the range reported previously for a variety of organic dyes,⁴ 0.92 ± 0.03 . In the tetrasubstituted case, VI, a higher T_g (90 vs 56 °C) with an improved morphological stability (*i.e.* absence of a recrystallization peak upon heating) was again accomplished. However, neither II nor VI was found to be liquid crystalline.

In an effort to create glass-forming materials capable of nematic mesomorphism, two previously reported high optical birefringence nematogenic precursors, 1-phenyl-2-(6-cyanonaphth-2-yl)ethyne²⁰ and cyanotolan,²¹ were

employed for the synthesis of **III**, **IV**, and **VII**. Note that all three systems exhibited nematic threaded textures under POM between T_g and T_c , the clearing temperature where a liquid crystalline mesophase undergoes a phase transition into an isotropic liquid, without detectable recrystallization peaks at a heating rate of 20 or 5 °C/min in DSC experiments, an indication of superior morphological stability to (–)-cholesterol and DR1 as pendant groups. In light of the stronger nematogen^{20,21} and the shorter spacer, it is little surprise that **III** possesses a higher T_g and a wider nematic mesophase temperature range than **IV**. A comparison of **VII** to **III** reveals that tetrasubstitution leads to a 30 °C elevation in T_g and a 71 °C increase in the nematic mesophase temperature range over disubstitution. On the basis of its rigidity and bulkiness, one might have expected adamantane with four pendant 1-phenyl-2-(6-cyanonaphth-2-yl)ethyne groups to show elevated thermal transition temperatures over 1,3,5-trisubstituted cyclohexane in a *cis-to-trans* molar ratio of 65/35, which was reported¹² to possess a T_g of 60 °C and a T_c of 197 °C. A comparison of the DSC data of **VII** to those of 1,3,5-trisubstituted cyclohexane¹² revealed a 17 °C elevation in T_g but a 7 °C depression in T_c . These results suggest that besides the structural disparity between the excluded-volume core and the pendant functional moiety, which was expected to be conducive to vitrification, apparent dimensionality of the hybrid system enforced by adamantane has emerged as an additional parameter that should be considered in molecular design.

IV. Summary

Novel molecular systems were synthesized by attaching (–)-cholesterol, nematogens, and DR1 to adamantane, which serves as an excluded-volume core for the formation of optically anisotropic and isotropic glasses. Specifically, systems containing (–)-cholesterol and nematogens exhibited smectic A/cholesteric and nematic mesophases, respectively, and those containing DR1 were found to be nonmesogenic. Although both di- and tetrasubstitution on adamantane with (–)-cholesterol and DR 1 were found to contribute to glass formation, tetrasubstitution resulted in systems with superior morphological stability, namely, an elevation in T_g and an absence of recrystallization upon heating the quenched glass. With nematogens 1-phenyl-2-(6-cyanonaphth-2-yl)ethyne and cyanotolan as pendant groups, morphological stability was accomplished in both di- and tetrasubstitution; however, tetrasubstitution was found to contribute to an elevation in T_g and an increase in the nematic mesophase temperature range. Compared to trisubstituted cyclohexane, tetrasubstituted adamantane gave rise to a somewhat elevated T_g but a somewhat depressed T_c , suggesting that the apparent dimensionality enforced by adamantane plays a role in

affecting vitrification and liquid crystal mesomorphism of the hybrid system.

Acknowledgment. We thank Professor A. S. Kende of the Chemistry Department at the University of Rochester for assistance in organic synthesis, Mr. K. L. Marshall and Dr. A. Schmid of the Laboratory for Laser Energetics for helpful discussions. We would like to express our gratitude to the Ministry of International Trade and Industry of Japan, Kaiser Electronics in San Jose, CA, for financial support of this research, and National Science Foundation for an engineering research equipment grant under CTS-9411604. Financial support provided by ARDEC to GEO-CENTERS, INC. is also gratefully acknowledged. In addition, our liquid crystal materials research was supported in part by the U.S. Department of Energy Office of Inertial Confinement Fusion under Cooperative Agreement No. DE-FC03-92SF19460, the University of Rochester, and the New York State Energy Research and Development Authority. The support of DOE does not constitute an endorsement by DOE of the views expressed in this article.

References and Notes

- (1) Adachi, C.; Tsutsui, T.; Saito, S. *Appl. Phys. Lett.* **1989**, *55*, 1489.
- (2) Haskal, E. I.; So, F. F.; Burrows, P. E.; Forrest, S. R. *Appl. Phys. Lett.* **1992**, *60*, 3223.
- (3) Roberts, G., Ed. *Langmuir-Blodgett Films*; Plenum: New York, 1990.
- (4) Naito, K.; Miura, A. *J. Phys. Chem.* **1993**, *97*, 6240.
- (5) Kreuzer, F.-H.; Andrejewski, D.; Haas, W.; Häberle, N.; Riepl, G.; Spes, P. *Mol. Cryst. Liq. Cryst.* **1991**, *199*, 345.
- (6) George, R. D.; Snow, A. W. *Chem. Mater.* **1994**, *6*, 1587.
- (7) Inada, H.; Shirota, Y. *J. Mater. Chem.* **1993**, *3*, 319.
- (8) (a) Attard, G. S.; Imrie, C. T. *Liq. Cryst.* **1992**, *11*, 785. (b) Attard, G. S.; Douglass, A. G.; Imrie, C. T.; Taylor, L. *Liq. Cryst.* **1992**, *11*, 779.
- (9) Wedler, W.; Demus, D.; Zschke, H.; Mohr, K.; Schäfer, W.; Weissflog, W. *J. Mater. Chem.* **1991**, *1*, 347.
- (10) Dehne, H.; Roger, A.; Demus, D.; Diele, S.; Kresse, H.; Pelzl, G.; Wedler, W.; Weissflog, W. *Liq. Cryst.* **1989**, *6*, 47.
- (11) Shi, H.; Chen, S. H. *Liq. Cryst.* **1994**, *17*, 413.
- (12) Shi, H.; Chen, S. H. *Liq. Cryst.* **1995**, *18*, 733.
- (13) Shi, H.; Chen, S. H. *Liq. Cryst.* **1995**, in press.
- (14) Mastrangelo, J. C.; Blanton, T. N.; Chen, S. H. *Chem. Mater.* **1995** submitted for publication.
- (15) Archibald, T. G.; Malik, A. A.; Baum, K. *Macromolecules* **1991**, *24*, 5261.
- (16) Reichert, V. R.; Mathias, L. J. *Macromolecules* **1994**, *27*, 7015.
- (17) Mathias, L. J.; Jensen, J. J.; Reichert, V. R.; Lewis, C. M.; Tullos, G. L. *Polym. Prepr.* **1995**, *36* (1), 1994.
- (18) Bashir-Hashemi, A.; Li, J.; Gelber, N. *Tetrahedron Lett.* **1995**, *36*, 1233.
- (19) Blanchard, P. M.; Mitchell, G. R. *Appl. Phys. Lett.* **1993**, *63*, 2038.
- (20) Hird, M.; Toyne, K. J.; Gray, G. W.; Day, S. E.; McDonnell, D. G. *Liq. Cryst.* **1993**, *15*, 123.
- (21) Wu, S.-T.; Ramos, E.; Finkenzeller J. *Appl. Phys.* **1990**, *68*, 78.

MA950587F